63-3-5

ARL 63-35

INFRARED SPECTRA AND TEMPERATURES OF PLASMAJETS:

SPECTROMETRIC AND SPECTRORADIOMETRIC MEASUREMENTS OF PLASMAJET TEMPERATURE DISTRIBUTIONS

LOWELL R. RYAN
HAROLD J. BABROV
RICHARD H. TOURIN

THE WARNER AND SWASEY COMPANY
FLUSHING, NEW YORK

FEBRUARY 1963

AERONAUTICAL RESEARCH LABORATORIES
OFFICE OF AEROSPACE RESEARCH
UNITED STATES AIR FORCE

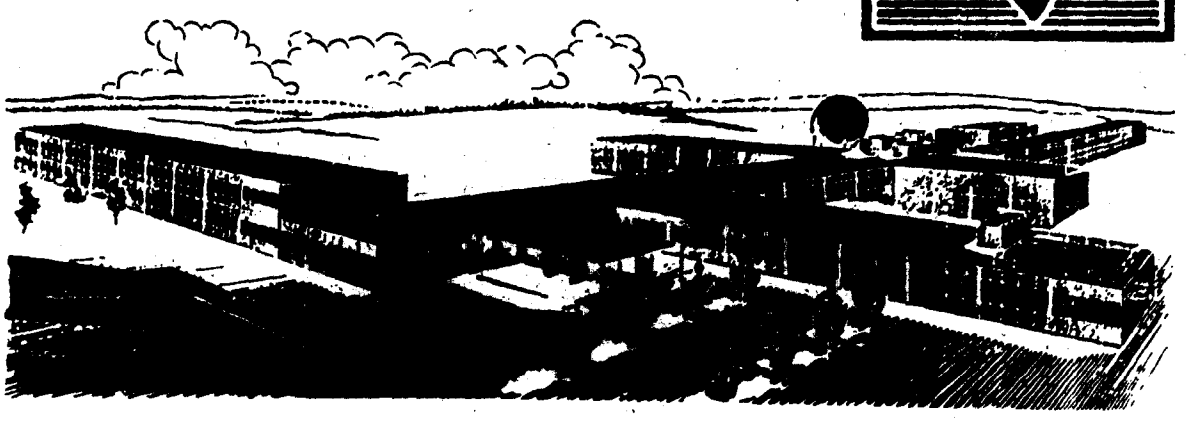

NOTICES

When Government drawings, specifications, or other data are used for any purpose other than in connection with a definitely related Government procurement operation, the United States Government thereby incurs no responsibility nor any obligation whatsoever; and the fact that the Government may have formulated, furnished, or in any way supplied the said drawings, specifications, or other data, is not to be regarded by implication or otherwise as in any manner licensing the holder or any other person or corporation, or conveying any rights or permission to manufacture, use, or sell any patented invention that may in any way be related thereto.

- - - - - - - - - - -

Qualified requesters may obtain copies of this report from the Armed Services Technical Information Agency, (ASTIA), Arlington Hall Station, Arlington 12, Virginia.

- - - - - - - - - -

This report has been released to the Office of Technical Services, U. S. Department of Commerce, Washington 25, D. C. for sale to the general public.

- - - - - - - - - - -

Copies of ARL Technical Documentary Reports should not be returned to Aeronautical Research Laboratory unless return is required by security considerations, contractual obligations, or notices on a specific document.

28-704, 400, 5-21-63

ARL 63-35

INFRARED SPECTRA AND TEMPERATURES OF PLASMAJETS:

SPECTROMETRIC AND SPECTRORADIOMETRIC MEASUREMENTS OF PLASMAJET TEMPERATURE DISTRIBUTIONS

LOWELL R. RYAN
HAROLD J. BABROV
RICHARD H. TOURIN

THE WARNER AND SWASEY COMPANY
FLUSHING, NEW YORK

FEBRUARY 1963

CONTRACT AF 33(616)-8057
PROJECT 7063
TASK 7063-01

AERONAUTICAL RESEARCH LABORATORIES
OFFICE OF AEROSPACE RESEARCH
UNITED STATES AIR FORCE
WRIGHT-PATTERSON AIR FORCE BASE, OHIO

FOREWORD

This interim technical report was prepared by the Warner and Swasey Co., Flushing, New York, on Contract AF 33(616)- 8057 for the Aeronautical Research Laboratories, Office of Aerospace Research, United States Air Force. The research reported herein was accomplished on Task 7063-01, "Research in Heat Transfer Phenomena" of Project 7063, "Mechanics of Flight" under the technical cognizance of Capt. Thiophilos Andrada of the Thermomechanics Research Laboratory of ARL.

The authors are grateful to Dr. M. P. Freeman, of the American Cyanamid Co., Stamford,Research Laboratory, for computing the Abelian integral inversions described in Section V, and for several helpful suggestions.

ABSTRACT

Temperatures of plasmajets were measured by several optical methods, and the results intercompared. Both spectrometric and spectroradiometric methods were used. Argon and nitrogen plasmajet temperatures were studied in particular detail. Large temperature gradients were observed in all the plasmajets studied. Spectra of plasmas were measured in both emission and absorption over the spectral range 0.37 to 5.0-μ. Substantial emission was observed throughout the entire region. All the plasmas proved to be optically thick (measurable absorption) in the region 0.7 – 2.0-μ and optically thin (no absorption) in the region 0.37 – 0.7-μ. An absorption-emission method of temperature measurement (the IMRA method), used in the absorbing region, and the single-line emission method, used in the visible, optically thin region, gave average temperatures along the optical path. The single-line measurements were always weighted more toward the peak temperature, while the weighting of the IMRA average varied with spectral wavelength, remaining consistently below the peak. The equivalence of the IMRA and single-line methods was shown for the limit of low absorption.

Radial temperature profiles in an argon plasmajet were studied by means of an Abelian integral inversion of lateral emission profiles measured for optically thin spectral lines. The results were compared to single-line temperatures measured along various chords through the plasmajet. The results of the two types of measurement were almost identical for short optical paths. For long paths the Abelian inversion gave consistently higher results, reflecting the large temperature gradient along the path. IMRA temperatures along a fixed path through the plasmajet varied with wavelength, reflecting the radial temperature profile.

A considerable amount of infrared absorptance was observed in a non-luminous region surrounding the visible plasmajet. Argon plasmajet temperatures ranged from 14,300°K down to 8000°K in the visible plasmajet, and from 8000°K to as low as 3000°K in the non-luminous zone. Nitrogen plasmajet temperatures ranged from less than 6000°K to 10,950°K on the axis. In an argon seeded nitrogen plasma close agreement was obtained between temperatures determined from the line intensities of atomic nitrogen and argon. The temperature from the argon line was based on an absolute intensity measurement, whereas the relative intensities of the nitrogen lines (Boltzmann plot) were used to determine the nitrogen temperature.

TABLE OF CONTENTS

LIST OF ILLUSTRATIONS

LIST OF SYMBOLS

A_{nm}	= Einstein's coefficient of spontaneous emission
B_{nm}	= Einstein's coefficient of induced emission
$B_{mn}=B_{nm}$	= Einstein's coefficient of absorption
B	= rotational constant
c	= speed of light
C_{em}	= emission constant for rotational line
e	= electronic charge
$\Delta\epsilon$	= ionization potential of atom
E_m	= energy of lower state
E_n	= energy of upper state
g_m	= statistical weight of lower state
g_n	= statistical weight of upper state
g_o	= statistical weight of ground state of atom
h	= Planck's constant
I_{abs}^{nm}	= intensity of absorption line
I_{em}^{nm}	= intensity of emission line
J	= rotational quantum number
k	= Boltzmann constant
L	= path length of emitter or absorber
λ_{nm}	= wavelength (cm) of line corresponding to n→m transition
m	= atomic mass
m_e	= electronic mass
n_e	= number density (cm^{-3}) of electrons
n_o	= number density (cm^{-3}) of atoms
n_1	= number density (cm^{-3}) of ions
N_m	= number density (cm^{-3}) of atoms in lower state
N_n	= number density (cm^{-3}) of atoms in upper state
ν_{nm}	= wavenumber (cm^{-1}) of line corresponding to n→m transition
Q_1	= partition function for ion
Q_o	= partition function for neutral atom
Q_r	= rotational partition function

INFRARED SPECTRA AND TEMPERATURES OF PLASMAJETS. II. SPECTROMETRIC AND SPECTRORADIOMETRIC MEASUREMENTS OF PLASMAJET TEMPERATURE DISTRIBUTIONS.

Lowell R. Ryan, Harold J. Babrov, and Richard H. Tourin

SECTION I.

INTRODUCTION

Infrared radiation of plasma arcs and plasmajets is of current interest because of its relation to heat transfer applications of plasma, fundamental studies of energy exchange in plasmas, and similar areas of research. Infrared techniques have proven particularly useful in plasma temperature measurements and their interpretation. Infrared emission and absorption spectra of argon, helium, and nitrogen plasmajets were measured in this laboratory (1-3)*, and temperatures were determined by the infrared monochromatic radiation (IMRA) method (4,5).

The measurement of plasmajet temperatures is hardly a straightforward, routine task. The lack of temperature standards in the range 3,000°K - 20,000°K makes it difficult to precisely define plasmajet temperatures or to determine absolute accuracy. In addition, plasmajets are never in complete thermal equilibrium. For this reason, one cannot readily specify the temperature of a plasmajet by a single number. The work described in this report was undertaken to help elucidate these problems. The consistency of plasma temperature measurements was studied by intercomparing several optical methods to measure plasma temperatures. While this did not eliminate the need for standards, it did help us to evaluate the measurement methods and to gain confidence in the results. The equilibrium problem was studied mainly in terms of radial temperature distributions in a plasmajet, measured by various methods. In this approach, one thinks of an inhomogeneous plasma as a series of relatively isothermal regions, each of which is in equilibrium. This is a mild sort of non-equilibrium; it is commonly symbolized LTE (Local Thermodynamic Equilibrium). With the aid of the LTE concept, it is quite reasonable and useful to measure plasma arc and jet temperatures. The existence of LTE is well-established for plasmas at pressures near atmospheric, at which the present work was done.

---

* Underlined numbers in parentheses refer to references listed at the end of this report.

All the methods of temperature determination used in this work involve an emission measurement along a chord through the plasma. Such a measurement, called "lateral emission", contains contributions from zones of different temperature. If the temperature gradient along a chord is large, the temperature calculated from the measured lateral emission will usually lie somewhere between the temperature extremes along the chord being observed. If the temperature distribution is radially symmetrical, with the highest temperature at the plasma axis, and if the plasma is non-absorbing (optically thin), then the lateral emission distribution, i.e. the emission measured along a series of parallel equidistant chords, can be transformed into a radial intensity distribution (and hence a radial temperature distribution) by means of an Abelian integral inversion (6). If radial symmetry does not prevail, or if the plasma is measurably absorbing (optically thick), the Abelian integral inversion cannot readily be applied*.

The plasma temperature studies described in this paper were based on emission and absorption spectra of argon, nitrogen, hydrogen, helium, and air plasmas, in the spectral region 0.37 - 5.0-μ. Most of the data were obtained in the 0.37 - 1.5-μ spectral region. The plasmas studied were usually optically thin in the visible and ultraviolet regions, while optically thick in the infrared.

SECTION II.

TEMPERATURE MEASUREMENT METHODS: THEORY

A. General

The methods we used to measure plasmajet temperatures may be grouped conveniently in two classes: spectrometric methods, which are based upon specific spectral features such as line shape, line width, intensity of a spectral line, etc.; and spectroradiometric methods, which depend upon the quantity of radiation at a given wavelength, but are independent of specific spectral features. Spectrometric methods apply to plasmas which are optically thin, where errors due to self-absorption are negligible. Spectroradiometric methods require that the plasma be measurably absorbing, or "optically thick". The Appendix contains a proof that in the limit, as absorption goes to zero, a spectrometric method - the "one-line" method - and a spectroradiometric method - the IMRA method - are equivalent. This is a very useful fact, as we shall see later.

---

* However, reference 7 describes an experiment whereby a modified form of the Abelian integral inversion may be applied if the absorption is weak.

B. Spectrometric Methods

1. The "one-line" method.

For an optically thin plasma, the expression for the integrated radiance of a spectral line is

$$I_{em}^{nm} = L \frac{c}{4\pi} N_n A_{nm} h\nu_{nm} \text{ erg sec}^{-1}\text{cm}^{-2}\text{sr}^{-1} \qquad (1)$$

where the subscripts n and m refer to the upper and lower energy states, respectively; A_{nm} is Einstein's coefficient of spontaneous emission (transition probability), N_n is the number density of atoms in state n, ν_{nm} is the frequency of the line in cm^{-1}, L is the path length, and h and c are the usual constants. N_n is given by the Boltzmann relation

$$N_n = n_o \frac{g_n}{g_o} e^{-E_n/kT} , \qquad (2)$$

where n_o is the number density of neutral atoms, g_n and g_o are the statistical weights of the upper state of the transition $n \longrightarrow m$ and the ground state, respectively; E_n is the energy of the upper state, k is Boltzmann's constant and T is the absolute temperature. Substituting Eq. (2) into Eq. (1), and substituting $\nu_{nm} = \lambda_{nm}^{-1}$, we have

$$I_{em}^{nm} = L \frac{hc}{4\pi} n_o \frac{g_n}{g_o} \frac{A_{nm}}{\lambda_{nm}} e^{-E_n/kT} \qquad (3)$$

If the wavelength λ_{nm} is expressed in microns and written λ_{μ}^{nm}, Eq. (3) can be written

$$I_{em}^{nm} = 1.582 \times 10^{-20} \frac{g_n A_{nm}}{\lambda_{\mu}^{nm}} n_o L \, e^{-E_n/kT} \text{ watts cm}^{-2}\text{sr}^{-1}, \qquad (4)$$

where the constants have been evaluated and the statistical weight of the ground state set equal to unity, as is the case for argon.

Equation (4) is useful only for spectral lines of known transition probability A_{nm}. The other quantities in Eq. (4) are readily known or easily determined constants, with the exception of the number density of neutral atoms n_o, which is a function of temperature.

The ideal gas law can be used to calculate n_o at temperatures where ionization is negligible. (Argon ionization is about 1% at 9,300°K). An iteration procedure must be used: one first assumes a temperature, calculates n_o from the ideal gas law, and substitutes the calculated value of n_o back into Eq. (4) to calculate the temperature. The process is continued until two successive calculations give the same result. This iteration converges quickly, because n_o varies much more slowly with T than does the exponential function in Eq. (4).

At temperatures higher than about 10,000°K, the ideal gas law is too inaccurate, and n_o must be determined from the Saha equation (8):

$$\frac{n_1 n_e}{n_o} = \frac{n_1^2}{n_o} = \frac{2(2\pi m_e kT)^{3/2} Q_1}{h^3 \quad Q_o} e^{-\Delta\epsilon/kT} \quad , \qquad (5)$$

where h, k and T have the usual meanings, n_e is the electron number density, n_1 is the ion number density, n_o is the neutral atom number density, m_e is the mass of the electron, Q_1 is the partition function of the ion, Q_o is the partition function of the atom, and $\Delta\epsilon$ is the ionization energy. Reference 9 contains a tabulation of n_o from 5,000°K - 18,000°K for argon, calculated from the Saha equation. From the table of reference 9, ionization of argon is 0.02% at 7,000°K, about 1% at 9,300°K, 2% at 10,000°K, and 10% at 12,000°K.

The line emission I_{em}^{nm}, given by Eq. (4), increases with increasing temperature until a maximum is reached at a temperature which depends on the particular atomic line (10). The maximum occurs when the effect of increasing temperature on the excitation of radiant emission is counterbalanced by the reduction in radiating species concentration due to ionization. For example, this temperature is 15,500°K for the 4158 Å argon line (10). If the temperature at the axis of the plasma is higher than that for which line emission is a maximum, the Fowler-Milne method, described in reference 10, is preferable to the one-line method, because it requires only a measurement of emission strength relative to the maximum, rather than an absolute measurement. The Fowler-Milne method was not used here, because the necessary condition was not fulfilled; the highest temperature observed in the argon plasma was about 14,500°K, whereas any visible neutral argon line reaches maximum intensity very near 15,000°K.

2. The two-line method (11).

If the transition probability, statistical weight of the upper state, energy of the upper state, and wavelength of each of two atomic lines are known, it follows from Eq. (3) that

$$\frac{I_1}{I_2} = \frac{g_1 A_1}{g_2 A_2} \frac{\lambda_2}{\lambda_1} e^{-(E_1 - E_2)/kT}$$

where the subscripts 1 and 2 refer to the two spectral lines.

Taking logarithms, we have

$$\ln \frac{I_1}{I_2} = \ln \left[\frac{g_1 A_1 \lambda_2}{g_2 A_2 \lambda_1}\right] - \frac{E_1 - E_2}{kT} \quad . \qquad (6)$$

In this case, one need not know the number density or path length, which are required for the one-line method. Moreover, one can use relative rather than absolute transition probabilities (12). A disadvantage of this method is that the calculated temperature is critically dependent upon the accuracy of the ratio of line intensities if the difference in upper energy states is small (say $|E_1 - E_2| < 0.4$ ev).

3. Atomic Boltzmann Plot (13).

The extension of the two-line method to many lines is called an atomic Boltzmann plot ("atomic" refers to the use of atomic constants). Recalling Eq. (3),

$$I_{em}^{nm} = L \frac{hc}{4\pi} n_o \frac{g_n}{g_o} \frac{A_{nm}}{\lambda_{nm}} e^{-E_n/kT} \quad .$$

Let $g_o = 1$ and take natural logarithms,

$$\ln \frac{I_{em}^{nm} \lambda_{nm}}{g_n A_{nm}} = \ln\left(L \frac{hc}{4\pi} n_o\right) - \frac{E_n}{kT} \quad .$$

Changing to base 10 and expressing E_n in units of $10^3 cm^{-1}$ for convenience in computation we get

$$\log \frac{I\lambda}{gA} = C - \frac{625E}{T} \quad ,$$

where

$$C = \ln(Lhcn_o/4\pi) \quad ;$$

and solving for T we have

$$T = \frac{625E}{\log \frac{I\lambda}{gA} - C} \quad . \qquad (7)$$

When $\log \frac{I\lambda}{gA}$ is plotted against E x $10^3 cm^{-1}$, the temperature is

given by the reciprocal of the slope. The constant C is chosen so as to express the ordinate in convenient units.

4. Molecular Boltzmann Plot (14).

If we assume the rigid rotator approximation, the expression for the intensity of a rotational line in a molecular vibration-rotation band is

$$I_{em} = \frac{C_{em}\nu^4}{Q_r} (J'+J''+1)e^{-B'J'(J'+1)hc/kT} ,$$

where C_{em} is a constant, ν is the frequency in cm^{-1}, J' and J" are the rotational quantum numbers of the upper and lower states respectively, B' is the rotational constant for the upper state, Q_r is the rotational partition function, T is the absolute temperature, and h, c and k are the usual constants.

Taking logarithms, we have

$$\ln \frac{I_{em}}{J'+J''+1} = A - \frac{B'J'(J'+1)hc}{kT} ,$$

where $A = C_{em}\nu^4/Q_r$.

For the R branch of the molecule N_2^+, this reduces to

$$\ln \frac{I_{em}}{2J'} = A - \frac{BJ'(J'+1')hc}{kT} \qquad (8)$$

The quantity $\ln \frac{I_{em}}{2J'}$ is plotted against $\frac{B}{k} J'(J'+1)hc$,

and the temperature is given by the reciprocal of the slope.

Use of the rigid rotator approximation entails two errors - that due to neglect of higher order terms in the energy, e.g. terms in $J^2(J+1)^2$, and that due to rotation-vibration interactions (15). No exact calculations have been made, but the effects are probably negligible for N_2^+ (16).

C. Spectroradiometric Methods

The methods described in the preceding section are applicable to a plasma which is optically thin. Where there is measurable absorption, these methods are no longer strictly valid, because spectrometric methods assume that radiation emerging from the plasma is the sum of the radiation emitted by each atom or

molecule along the optical path in the plasma. This condition obviously is not fulfilled if the constituents of the plasma show appreciable absorption at the radiation frequencies.

The presence of absorption allows the Kirchhoff relation to be used:

$$\frac{W_\lambda(T)}{\alpha_\lambda(T)} = W_\lambda{}^b(T) \quad , \qquad (9)$$

where $W_\lambda(T)$ is the measured spectral emittance, α_λ is the measured spectral absorptance, and $W_\lambda{}^b(T)$ is the Planck function,

$$W_\lambda{}^b(T) = c_1\lambda^{-5}(e^{c_2/\lambda T}-1)^{-1}$$

This principle of temperature measurement has been investigated extensively and applied to gas temperature measurement in flames and shock waves, as well as in plasmas (4,5), in a form referred to as the infrared monochromatic radiation (IMRA) method.

Equation (9) holds for a homogeneous region in equilibrium. When temperature gradients exist, the plasma as a whole is no longer homogeneous. However, it is not necessary that the entire plasma be in equilibrium for the IMRA method to be valid, but only that local thermodynamic equilibrium (LTE) exist within volumes whose dimensions are small compared with that of the plasma as a whole. Emission and absorption measurements across the plasma will contain contributions from all portions of the plasma which lie along the optical path. The temperature determined from the emittance/absorptance measurements at each wavelength is a weighted average of the temperatures along the optical path. The variation with wavelength perhaps can lead to a knowledge of the temperature profile along the path. Such average temperatures are potentially useful to represent the thermal state of the plasma as a whole. This subject is currently under active study; much remains to be done to realize in practice the advantages of this method of plasma temperature measurement.

SECTION III.

APPARATUS

A. Plasmajet Equipment

The plasma equipment used for the work described in this report was substantially the same as that described in

reference 3, but a number of significant changes were made.

Figure 1 is a cross section of the plasmajet nozzle and electrode. The arc is struck between the water-cooled tungsten electrode and the inner surface of a water-cooled hollow copper cylinder. The gas to be studied is forced under pressure through the annulus between the two electrodes, across which can be applied various open circuit voltages (80v, 160v, and 320v were sufficient for our purposes). For starting, a high frequency voltage (about 6,000v) is momentarily impressed between the electrodes, and a self-sustaining arc is formed, after which the voltage between the electrodes drops to about half the open circuit voltage. The arc-heated, partially ionized gas flows through the nozzle and emerges from the orifice as a brilliant "flame". Two Thermal Dynamics PLC-12.5 selenium rectifiers were added as power supplies. These rectifiers are essentially Miller SRH-444 DC arc welding units, which have been modified so that open circuit voltages of 80v, 160v, and 320v can be selected. Two nozzles, one of 7/32" I.D. and the other of 5/16" I.D., were used in the work described in reference 3 for all plasmas.

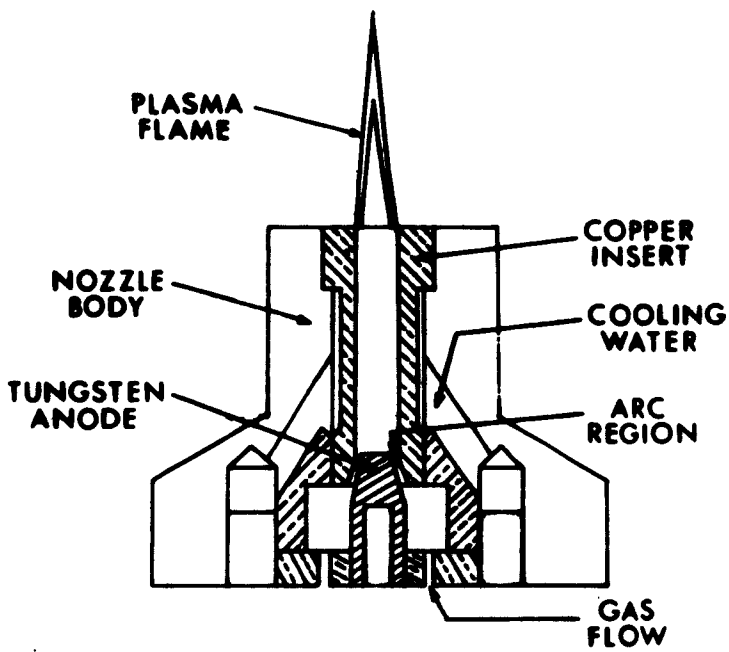

Fig. 1. Cross section of plasmajet nozzle.

Figure 1 is a cross section of the 7/32" I.D. nozzle. More recently, special high enthalpy, laminar flow nozzles, which produce a very stable flame, have become available for use with argon and helium. The central portion of one of these nozzles consists of a removable insert which can readily be changed in case of burnout. If standard size high pressure cylinders are used as gas supply for argon and helium, the plasma can be maintained for several hours, because the flow rates required with these nozzles are considerably less than with the nozzles formerly used. For the air plasma, a special nozzle with a replaceable insert of 3/16" throat diameter was used. Although a high flow rate was required, the air plasma produced with this nozzle was more stable than could previously be obtained. Because the air plasma causes rapid erosion at the nozzle orifice, the readily replaceable insert is a considerable advantage. It was found that the air nozzle also produced a satisfactory nitrogen plasma without erosion and with minimum likelihood of burnout. The hydrogen plasma was produced with one of the older nozzles (7/32" I.D.) used in the work reported in references 1 and 2. Because standard size high pressure cylinders were used to supply the hydrogen, and because a very high flow rate is required, the hydrogen plasma could be maintained for only about ten minutes.

The argon and helium plasmas appear very similar to the eye. Each consists of an outer cone about 0.2" in diameter at the base and about 1¼" in height, and a more intense coaxial inner cone of slightly smaller dimensions.

Power input and flow rate were adjusted so as to produce a plasma of maximum stability. In general, there is a range of flow rates and power input for each gas which produce a suitable plasma. A particular combination of flow rate and power input was selected for each gas, within this range. These operating conditions were as follows: argon - 400 amp, 25v (10 kw), 20 SCFH; helium - 300 amp, 48v (14.4 kw), 104 SCFH; hydrogen - 160 amp, 140v (20.8 kw), 1000 SCFH; nitrogen - 120 amp, 140v (16.8 kw), 80 SCFH; air - 50 amp, 300v (15 kw), 250 SCFH.

B. Optical and Electrical Instrumentation

A schematic diagram of the optical system used is shown in Fig. 2. The system consists of three separate units, each having its own housing: the source unit, receiver unit, and monochromator. Radiation from the source G (globar or tungsten strip lamp) is reflected from flat mirror M_1 to spherical M_2, leaves the source unit through a hole in the cover, and is focused at the plasma. Radiation from this point (either from the source or from the plasma) diverges and enters the receiver unit where it is reflected from movable flat mirror M_3 to spherical mirror M_4 to flat mirror M_5. The converging beam leaves the receiver and

enters the monochromator, coming to a focus at the entrance slit. The receiver unit also contains a standard strip lamp, used for quantitative calibration of the plasma radiation. When the flat mirror M_3 is rotated into the position indicated by the dashed lines, radiation from the strip lamp is reflected from this mirror and is focused on the entrance slit of the monochromator via M_4 and M_5 as before. The monochromator is a Perkin-Elmer Model 98; the well-known optical path between the entrance slit and the exit slit is shown in Fig. 2. When the 45° flat mirror M_6 is in place behind the exit slit, radiation will be reflected to the ellipsoid mirror M_8 and focused on the bolometer detector, which replaced the standard thermocouple. With the flat mirror M_6 removed, the beam diverges until it is reflected by spherical mirror M_7, which is outside the monochromator, and focused on a PbS detector. On occasion, the flat mirror M_6 was also replaced by a photomultiplier (1P21) such that the radiation emerging from the exit slit fell on the sensitive surface.

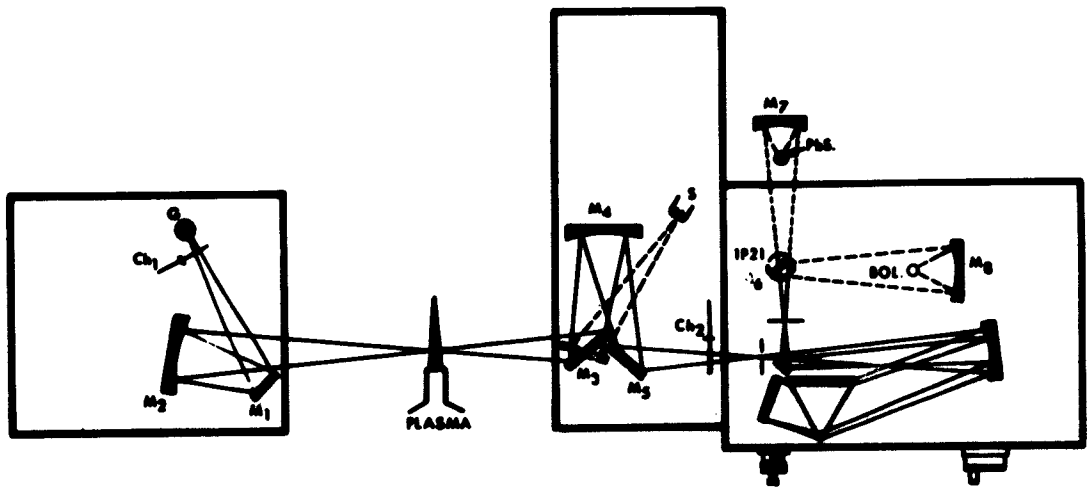

Fig. 2. Schematic of optical system.

The system contains two 90 cps choppers, Ch1 and Ch2, one placed near the source and the other at a point just before the beam leaves the receiver unit. Each chopper is mounted such that the beam is intercepted at a point directly below the axis of the blade. A small lamp and photo-pickup are mounted above the axis on opposite sides of the blade. Thus, the lower blade begins to

chop the optical beam when the upper blade begins to chop the beam to the photo pickup. The choppers modulate the radiation beam, so that the detector outputs can be amplified by an AC amplifier. By alternately using choppers 1 and 2 absorption and emission of the plasma are measured independently. The signal from the AC amplifier is synchronously rectified by means of a synchroverter activated by the photo-pickup, and the DC output is read on a strip-chart recorder. The assembly holding the lamp and photo-pickup can be moved along an arc concentric with the chopper blade, which allows the system to be phased. By removing the shutter at the source and comparing the signal using one chopper with that using the other, the two photo-pickup assemblies can be phased such that the use of either chopper produces the same signal. There are two independent gain controls, one used when the globar (or strip lamp) in the source unit is the source of radiation, the other when the plasma or the calibrating strip lamp in the receiver unit is the source.

The plasma torch was mounted on a compound table, which in turn was mounted on an elevator table. Thus, the plasma could be moved along any of the three Cartesian coordinates. Motion in the xy plane (horizontal) is provided by the compound table, and motion in the z direction (vertical) is achieved with the elevator table. The compound table is mounted such that one coordinate is parallel to the optical axis; this coordinate is used only to focus the plasma. The plasma may then be traversed in a horizontal plane perpendicular to the optical axis.

All plasmas were operated such that the plasma axis was vertical. Since the monochromator slits were also vertical, the axes of the plasma image and the monochromator slits were always parallel. Certain experiments cited in reference 3 showed that a strong axial temperature gradient existed in the plasma. By masking the entrance slit, the effective slit height was decreased from $\frac{1}{2}$" to 1/6", thus reducing the temperature range due to axial gradients.

SECTION IV.

MEASUREMENTS OF PLASMA SPECTRA

A. General

By a suitable choice of prism and detector, the spectral region from 0.37 - 5.0-μ was studied. For the spectral region 0.37 - 0.65-μ a glass prism and 1P21 photomultiplier were used; for 0.65 - 2.0-μ a glass prism and lead sulfide detector; and from 2.0 - 5.0-μ a lithium fluoride prism and bolometer. The 0.37 - 1.5-μ spectral region has the greatest line density and line intensity, hence it is the region in which most observations

were made. The 0.37 - 0.65-μ region closely corresponds to the visible region of the spectrum and is therefore referred to as the "visible". The longer wavelength region is, of course, the "infrared".

B. Visible Region (0.37 - 0.65-μ)

1. Argon, Helium, Hydrogen Emission Spectra

Visible spectra of the neutral atom were identified for each of the monatomic gases studied. No spectra of ionized species were observed. Figure 3 is a tracing of the spectrum of a helium plasma; the lines are those of the neutral helium atom. Similarly, the argon plasma spectrum consists solely of neutral atomic lines.

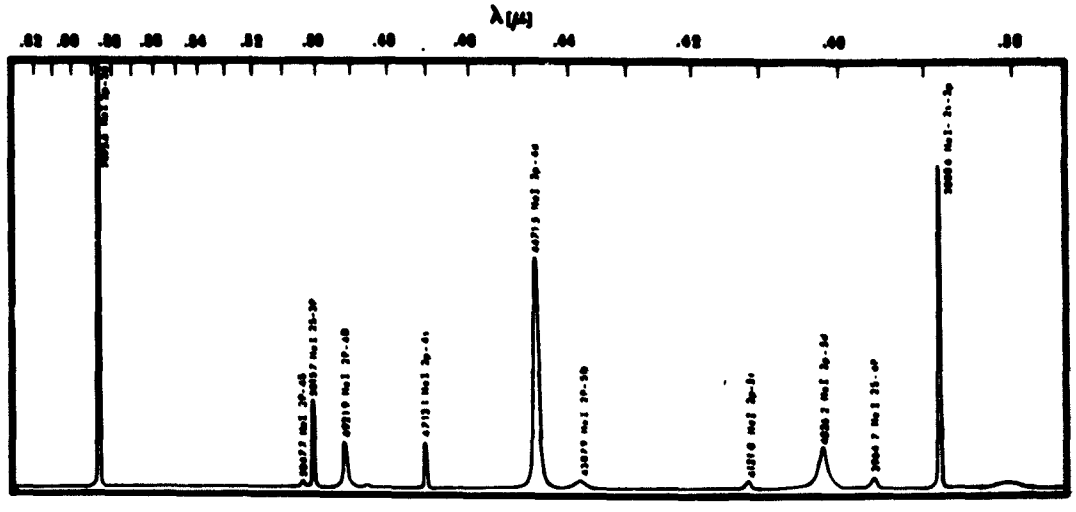

Fig. 3. Spectrum of helium plasma.

The hydrogen spectrum consisted of the H_α, H_β, H_γ, and H_δ lines of the Balmer series. The argon and helium spectra were taken under varying conditions of flow rate and power input, at various heights above the nozzle and under high amplification, but no lines were seen at wavelengths corresponding to the strongest lines of the ion spectra. It is therefore concluded that the population of ions in excited states is negligible, but, as will be shown later, this does not mean that the population of ions in the ground state is negligible.

2. Nitrogen Emission Spectrum

Figure 4 shows two nitrogen plasmajet spectra over the same spectral region but at different distances above the nozzle. The upper curve corresponds to a spectrum along a diameter 3/8" above the nozzle; the lower curve corresponds to a spectrum along a diameter 3/4" above the nozzle. The lower spectrum consists mainly of several bands of N_2^+, most prominently the $N_2^+(0,0)$ and $N_2^+(1,1)$ bands at 3914.4 Å and 3884.3 Å respectively. Immediately to the right of the $N_2^+(1,1)$ band head the rotational lines of the $N_2^+(0,0)$ band can clearly be seen.

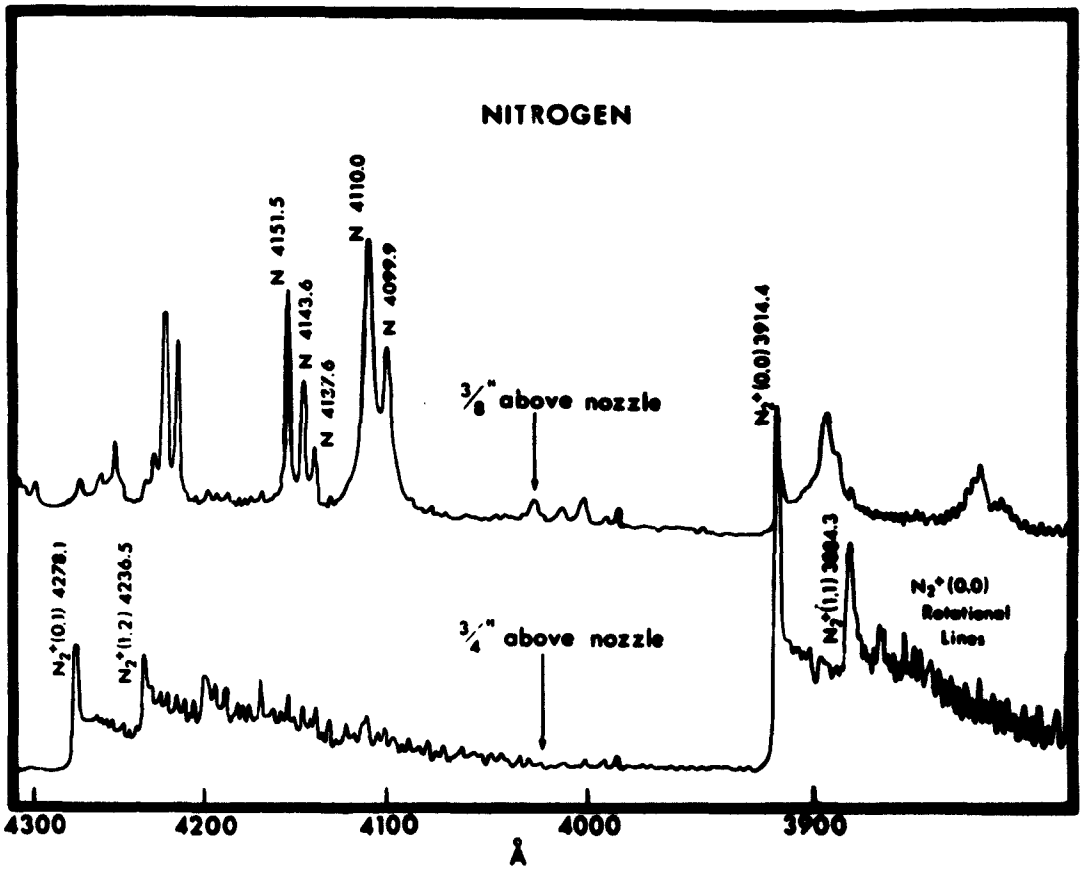

Fig. 4. Spectra of a nitrogen plasma, at different points on the plasma axis.

The structure extending from the $N_2^+(0,1)$ band head at 4278.1 Å to about 4000 Å is a mixture of N_2^+ band heads, rotational lines and atomic lines of nitrogen. In the upper spectrum, the atomic lines are considerably stronger relative to the molecular N_2^+ bands. Here, the N_2^+ system is obscured by the appearance of two unidentified band heads.

Several spectra were obtained at 3/8" above the axis along parallel chords at increments of 0.01" from a diameter. Examination of these spectra showed that as one moves from the axis toward the boundary, the intensities of the atomic lines decrease and the intensity of N_2^+ increases until near the boundary the spectrum appears very similar to that of Fig. 4 at 3/4" above the nozzle. These variations of radiating species obviously correspond to large axial and radial temperature gradients.

Figure 5 is a tracing of a section of the $N_2^+(0,0)$ spectrum at a position 3/4" from the nozzle. The separation of the rotational lines is about 3 Å, which is somewhat less than could accurately be determined by means of the wavelength calibration curve of the monochromator. To assure positive identification of the N_2^+ rotational lines, an argon plasma spectrum was superposed on the N_2^+ spectrum, and the 3850.6 Å and 3780.8 Å argon lines were used as calibration points. Comparison of these wavelengths with the calculated positions of the N_2^+ rotational lines allowed rotational quantum numbers to be assigned.

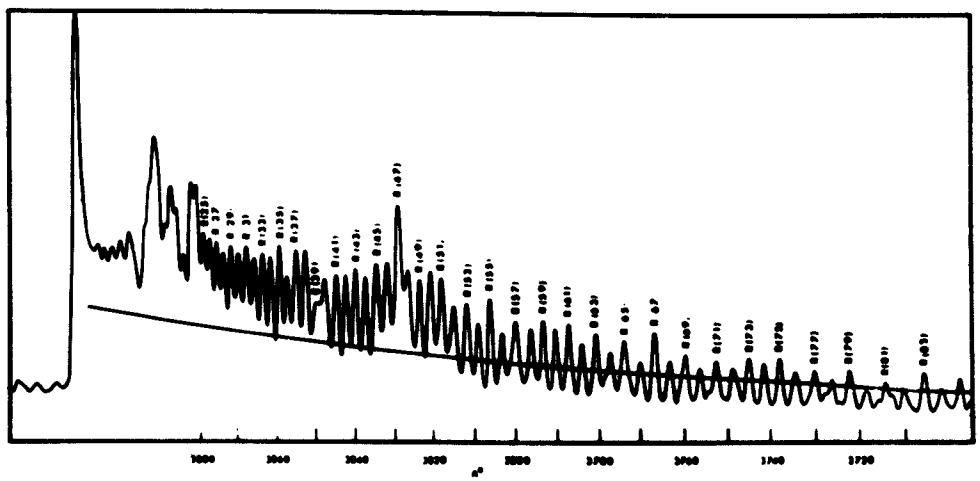

Fig. 5. N_2^+ spectrum, measured in a nitrogen plasmajet. The continuous spectrum in the lower part of the figure is the strip lamp emission.

The spectrum of an air plasma along a diameter 3/8" from the nozzle is similar to that of a nitrogen plasma at the same point. N_2^+ is very weak relative to the lines of atomic nitrogen, and in this case, of atomic oxygen. Many operating difficulties make the air plasma much more difficult to study than the nitrogen plasma. A secondary arc strikes from the plasma to the nozzle, causing rapid erosion. The arc rotates erratically about the central plasma, making off-axis measurements optically "noisy".

3. Absorption Studies.

A continuous source was placed behind each plasma in an attempt to obtain an absorption spectrum. However, none of the plasmas exhibited either line or continuum absorption spectra in the visible region. A more sensitive check for absorption was performed by reflecting an image of the plasma back on the plasma itself (3). The results confirmed that the plasmas studied are optically thin in the visible region.

C. Infrared Region (0.65 - 2.0-μ)

The infrared spectra observed are extensions of the visible spectra and, as expected, one sees lines of the neutral atom. One striking difference between the visible and infrared regions is the occurrence of absorption spectra in the latter.

The transition from optically thick to optically thin spectral regions is evident in Fig. 6, which shows infrared emission and absorption spectra of argon. The upper curve of this figure is the spectrum of a continuous source behind the plasma-jet. The curve lying immediately below the upper curve is the absorption spectrum of the argon plasma, which consists of a superposition of atomic lines and continuum. The lowest curve is the emission spectrum. At 0.65-μ, the absorption continuum is immeasurably low. Absorption becomes appreciable between 0.65-μ and 0.70-μ, and increases with increasing wavelength, reaching a maximum near 1.50-μ. From 1.70-μ to about 0.82-μ emission and absorption are roughly proportional. At wavelengths shorter than 0.82-μ, absorption begins to decrease. The strong line at 0.77-μ, for instance, shows less absorption than lines of similar strength at longer wavelengths. The line at 0.75-μ shows much less absorption, and the line at 0.74-μ almost none. Figure 7 is a plot of absorptance vs wavelength (dashed curve), and the ratio of emittance to absorptance $W_\lambda(T)/\alpha_\lambda(T)$ vs wavelength (solid curve). The vertical dotted line at 0.675-μ corresponds to the minimum wavelength at which there is measurable absorption, i.e. the point at which absorptance goes to zero. These results were checked by the reflection method discussed above, in which the spherical mirror in the source unit was placed so that the plasma was focused back on itself.

Emissivities calculated by this method for several spectral lines were 10 - 20% higher than those calculated by using a continuous source, but the above results are verified: lines of wavelength less than 0.675-μ have immeasurably low emissivities; lines of wavelength greater than 0.675-μ have measurable emissivities.

The argon plasma flame has been described as nearly conical, $1\frac{1}{4}$" high and about 0.2" in diameter at the base near the nozzle; therefore a position 0.1" off axis corresponds to the visible plasma boundary. Absorption measurements were made as far as two plasma radii from the axis, beyond the visible boundary, and the absorption was still measurable, indicating the presence of argon in excited states. This is probably argon which has diffused out of the plasma. Since the corresponding emission was extremely low, populations in excited states must be considerably lower here than in the luminous cone of the plasma.

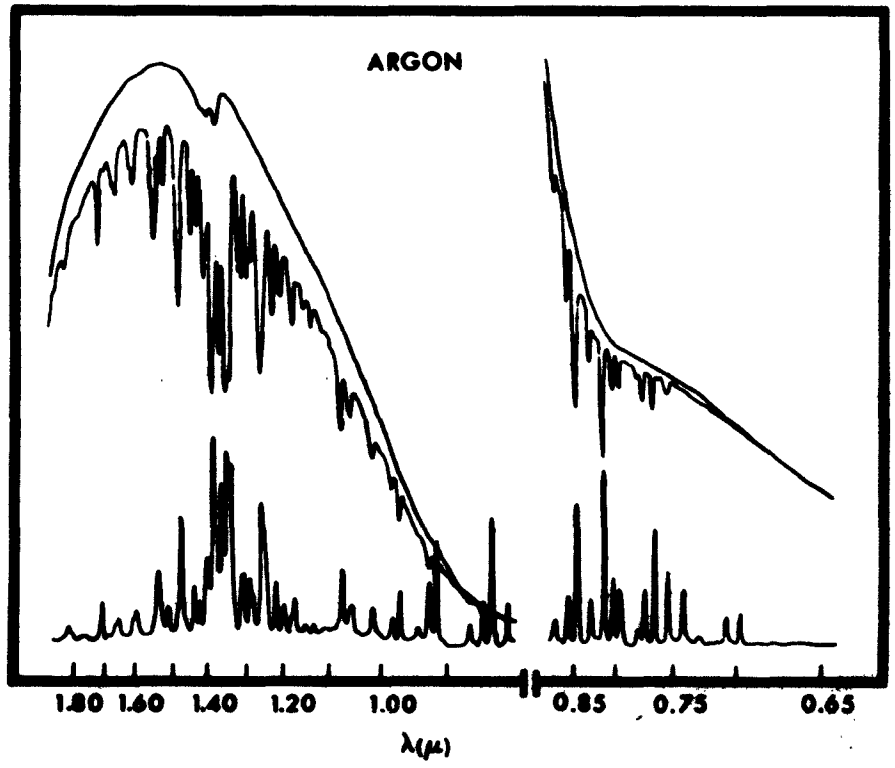

Fig. 6. Emission and absorption spectra of argon.

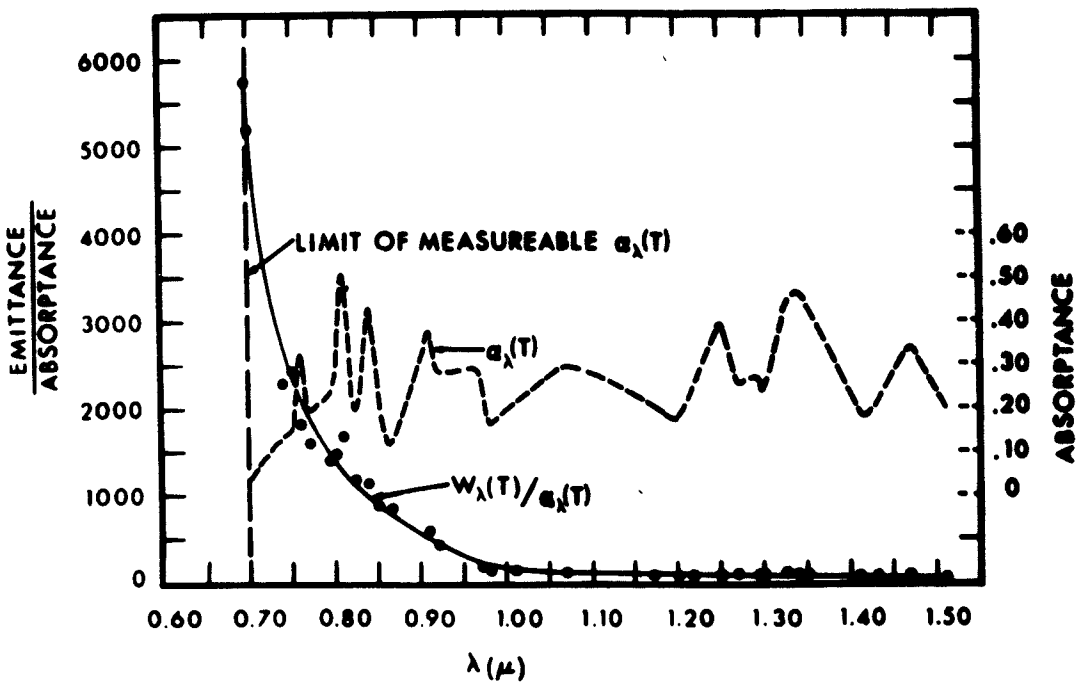

Fig. 7. Spectral absorptance and emittance/absorptance ratios of an argon plasma.

The hydrogen, helium, nitrogen, and air plasmas also showed measurable absorption in the infrared. Absorption of those gases will be discussed in the following section.

A continuum was observed in all the infrared spectra measured. This continuous radiation is due to electron-ion recombination (free-bound electron transitions) and Bremsstrahlung (free-free electron transitions in the field of an ion). Hence there must be ions present in the plasma. The fact that no ion spectra were observed indicates that the populations of excited states of the ions are negligible relative to the populations of excited states of the neutral atoms. This appears reasonable, because the first excited states of ions lie considerably above the ion ground state. For example, the first excited state of the argon ion lies 13.5 ev above the ground state. From the Saha equation (Eq. 5), one finds that at 12,000°K the population of Ar II (singly ionized argon) is about

10% of the total population. The population of Ar III at this temperature is of the order 4×10^{-6} that of the total population.

SECTION V.

PLASMA TEMPERATURE MEASUREMENTS

A. General

Plasmajet temperatures were determined by the methods outlined in Section II. In the spectroradiometric (IMRA) method, an emission spectrum, absorption spectrum and continuous background spectrum were obtained. A fourth spectrum, that of the calibrating strip lamp, was measured also, which enabled relative emission to be converted into spectral radiance (watts cm^{-2} μ^{-1}).

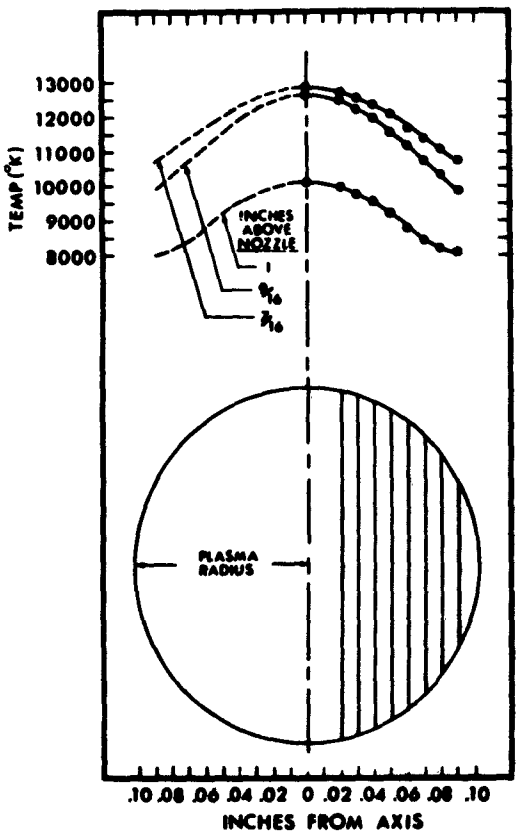

Fig. 8. Lateral temperature distribution in an argon plasma, measured by the single-line method.

When applying the spectrometric methods, the area under a given spectral line was compared to the area of equal width under the spectrum of the calibrating strip lamp, to obtain the radiance of the line.

B. Argon

The 4300 Å line is one of the most intense argon lines for which the transition probability is known, and it was well resolved in our measurements. The radiance of this line was measured along various horizontal chords from a diameter to the outer boundary of the plasma, in increments of 0.01", at three different heights above the nozzle opening. Temperatures were calculated from the measured radiances by means of the one-line method. The results are shown in Fig. 8, where temperatures are plotted against off-axis position for heights of 7/16", 9/16" and 1" above the nozzle. A plot of temperature vs off-axis distance, as in Fig. 8, is referred to as a lateral profile. The lower part of Fig. 8 shows a cross-section of the plasma taken perpendicular to the axis; the chords correspond to the principal ray of each observation. The intensity of a spectral line measured along one of these chords contains contributions from all points along the chord. From Eq. (4), the expression used to convert radiance to temperature, we see that radiance is a very sensitive function of temperature; i.e. we should expect a small relative difference in temperature to correspond to a large relative difference in radiance. For example, a calculation based on the 4300 Å argon line shows that the radiation from a uniform zone of plasma at 8780°K is only 1% of that from a uniform zone at 12,000°K. If there is a large temperature gradient along a given chord, we therefore expect the calculated temperatures to be weighted strongly toward the highest temperature which exists along the chord.

In order to determine the experimental error in the one-line method, temperatures were calculated from several lines for which the transition probabilities are known. Table I shows the results of a series of temperature calculations from several lines of an argon plasma at an on-axis point 3/4" above the nozzle opening. The transition probabilities for these lines are given (17) to 20% accuracy; the measurement of the line width might be in error by 5%. Combining these errors and calculating temperature limits from the 4300 Å argon line we get T_{min} = 11,050°K, T_{max} = 11,420°K. This result is consistent with the experimental results shown in Table I.

TABLE I.

Argon Plasma Temperatures Determined by the One-Line Method

λ	T
4300 Å	11,250°K
4272	11,000
4266	11,370
4259	11,200
4158	11,050
4164	11,050

average: 11,210 ± 160°K

To check whether the plasmajet was radially symmetrical, the monochromator was set at the 4300 Å argon line, and the relative emission noted at various distances from the plasma axis. Figure 9 shows a plot of relative emission against distance from the plasma axis, measured 7/16" above the nozzle opening. Since the plasma was radially symmetrical, an Abelian integral inversion could be applied (7) transforming the lateral radiance measurements into radiance as a function of radius. The corresponding temperatures were calculated, and these temperatures were plotted versus radial distance from the plasma axis. The results are shown in Fig. 10, where the data of Fig. 8 are also plotted for comparison. The data corresponding to the distance 1" from the nozzle were not inverted. The lines of the argon infrared spectrum discussed in Section IV were used to make a series of IMRA (4) temperature measurements. These temperatures were plotted against wavelength, as shown in Fig. 11. Temperature is seen to increase monotonically with decreasing wavelength, from 2,700°K at 1.5-μ to 8,000°K at 0.7-μ. To see why temperature is not constant with changing wavelength, consider Fig. 7 again. If the temperature and emissivity of the plasma were uniform, the plot of $W_\lambda(T)/\alpha_\lambda(T)$ vs wavelength would be a blackbody curve characteristic of the temperature T. It is evident that the solid curve in Fig. 7 is not a blackbody curve, but rather becomes steeper than a blackbody curve with decreasing wavelength. The data in Figs. 7 and 11 are in accord with the existence of a temperature gradient as shown in Fig. 10.

The relationships shown in Figs. 7, 10, and 11 may perhaps be better understood if one considers the nature of the Planck function, $N_\lambda^0(T)$. Suppose that the plasma temperature is 12,000°K at the axis and 8,000°K at the boundary. Figure 12 shows the Planck function as a function of wavelength for these two temperatures.

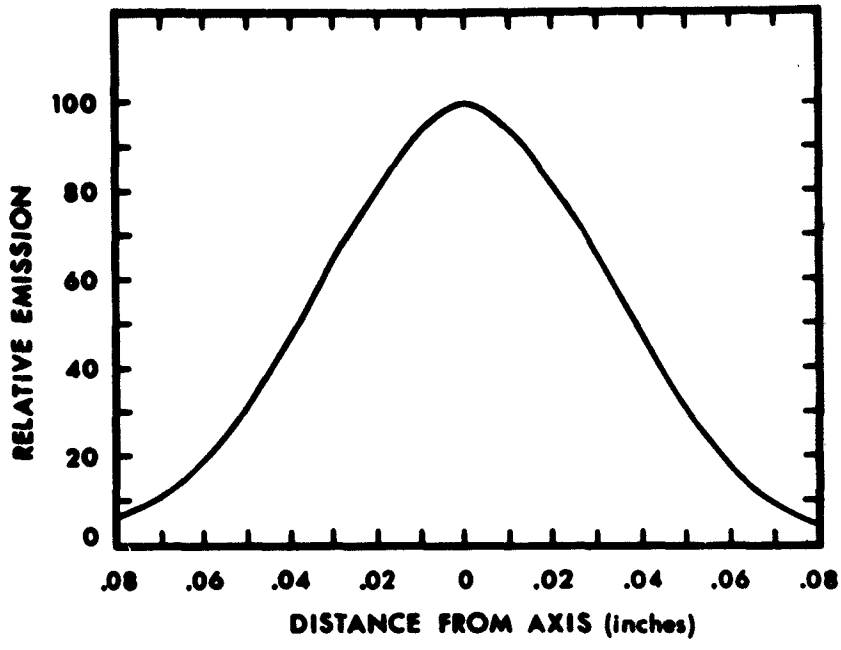

Fig. 9. Intensity profile of argon 4300 Å line.

At longer wavelengths, where absorption is high (recall that there is appreciable absorption outside the luminous cone of the plasma) much of the radiation from the high temperature zone near the axis is reabsorbed, hence the radiation reaching the detector is lowered. As the wavelength decreases, the radiation from near the axis is rapidly increasing. At wavelengths shorter than 0.80-μ, the absorptance is rapidly going to zero (see Fig. 8) and correspondingly more of the radiation from near the axis is reaching the detector. Therefore, we should expect the temperatures measured at shorter wavelengths, which are determined spectrometrically, to be strongly weighted toward the peak. A lateral series of such measurements along various chords should give a good representation of the radial temperature distributions near the boundary of the luminous portion of the plasmajet, while an Abelian integral inversion of the lateral profile gives a better representation near the axis. We should also expect the

spectroradiometric (IMRA) measurement, made at the longer wavelengths, to give weighted mean temperatures.

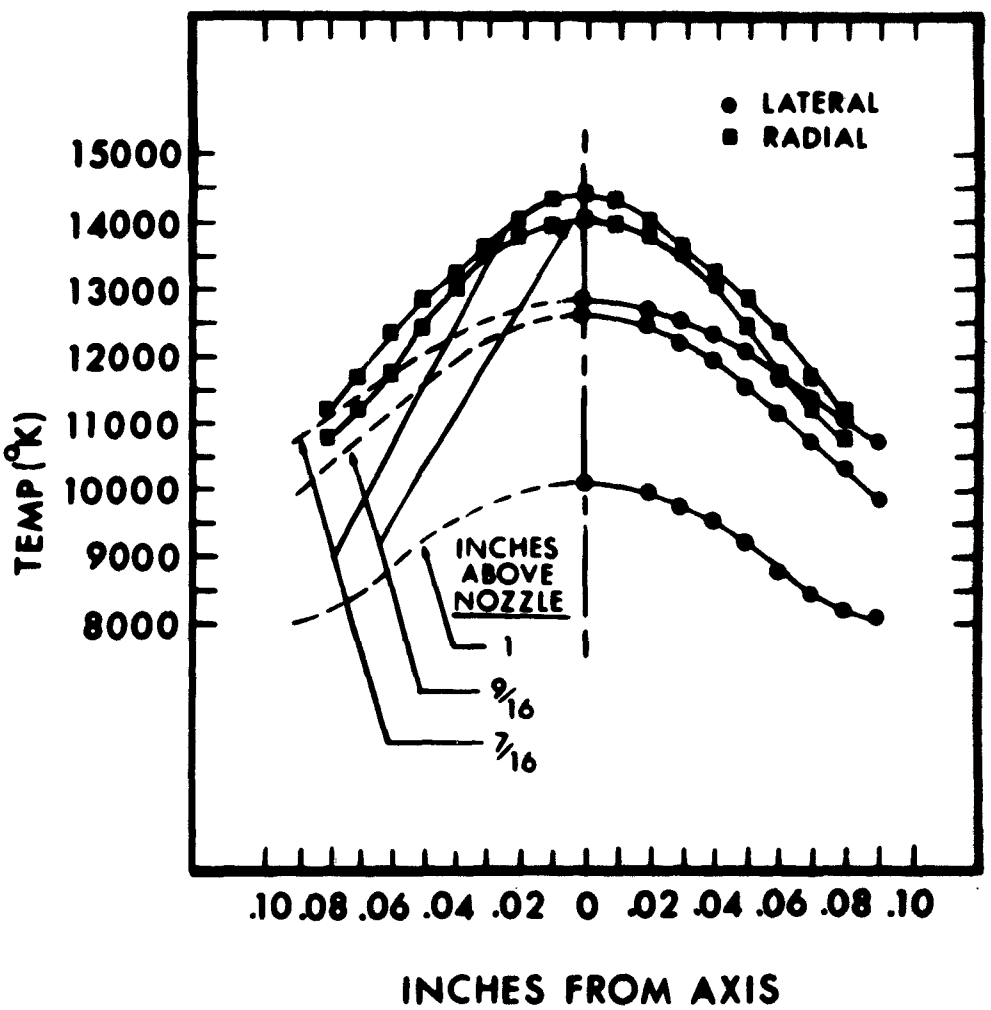

Fig. 10. Lateral and radial temperature distributions in an argon plasma , measured by the single-line method and by Abelian integral inversions.

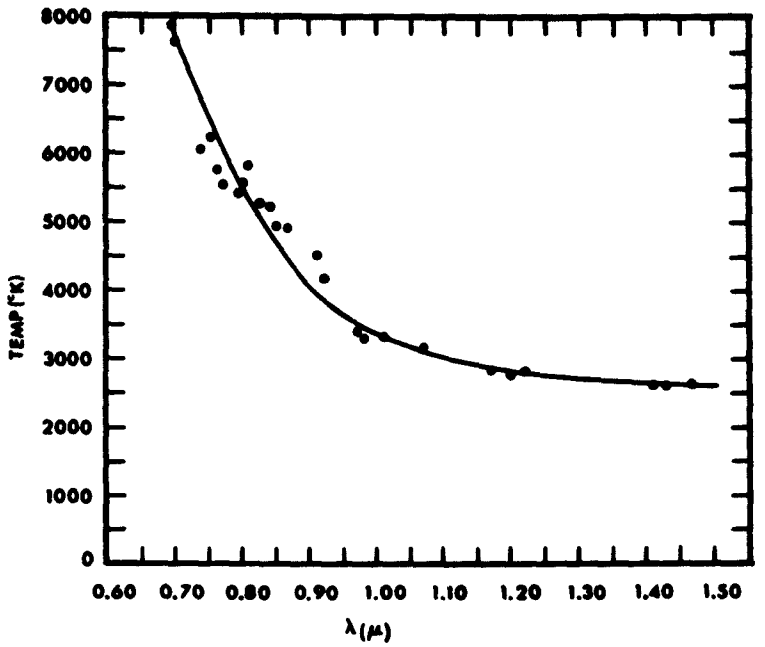

Fig. 11. IMRA temperatures of an argon plasma, measured at 7/16" above the nozzle.

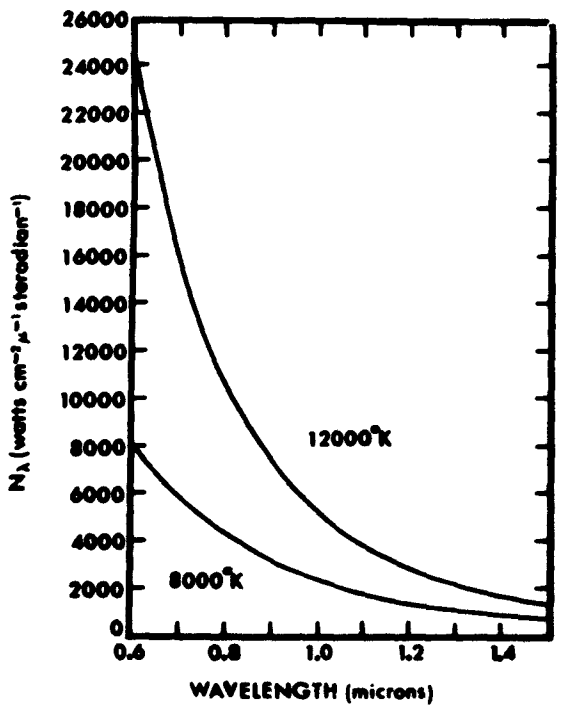

Fig. 12. Blackbody radiance curves.

C. Nitrogen

Neutral atomic nitrogen and N_2^+ were shown in Section IV to be the constituents contributing to the nitrogen plasma spectrum. As was the case with the argon plasma, there are pronounced radial and axial temperature gradients. As will be shown, the temperatures in the nitrogen plasma vary from 6,000° to 11,000°K.

There is considerably more difficulty involved in applying the one-line method to nitrogen than to argon. For argon, one need only consider the ionization, from neutral atom to ion at a given temperature, and this can be calculated from the Saha equation. The neutral nitrogen molecule, however, yields neutral atomic nitrogen, nitrogen ions, and N_2^+. The task of calculating the concentration of neutral nitrogen atoms over the temperature range of the plasma is formidable. For this reason, the one-line method was not applied to nitrogen. Other spectrometric methods were used to measure nitrogen plasma temperature. The two-line method was tried, since it does not require a knowledge of number density. Temperatures calculated from several pairs of nitrogen lines differed from one another by an amount considerably greater than that which could be accounted for as experimental error or error in the transition probabilities (18). Since the temperature calculated by this method is critically dependent upon the ratio of line intensities, the presence of an unresolved line lying under one of the lines used in the measurement could cause a large error. A Boltzmann plot, which is the best straight line fit to points plotted according to Eq. (7) of Section II, tends to average out such errors. Figure 13 shows a plot for six nitrogen lines measured on the plasma axis 3/8" above the nozzle. The temperature of 10,750°K shown on the figure was calculated from the slope of the line. As an independent check of this temperature, the plasma was seeded with just enough argon to obtain argon lines of sufficient intensity to be measured. The resulting "one-line" temperature was 10,930°K, in good agreement with the atomic Boltzmann plot.

Recall from Fig. 4 that 3/4" above the nozzle, the N_2^+ emission appears strong and the atomic nitrogen lines are weak (too weak to be used for an atomic Boltzmann plot). At 3/8" above the nozzle, the atomic lines are strong and the rotational lines of N_2^+ are weak. At 9/16" above the nozzle, midway between these points on the axis, both atomic lines and N_2^+ lines are strong enough to be used. Figure 14 shows a molecular Boltzmann plot made from the rotational lines of N_2^+ measured 9/16" above the nozzle opening; the temperature obtained from the slope of the line is 6,380°K. A Boltzmann plot made from the nitrogen atomic lines is shown in Fig. 15, and indicates a temperature of 8,950°K. This plasma was also seeded with argon, from which a one-line

temperature of 8,960°K was calculated, again confirming the atomic Boltzmann plot. If, as it appears, the temperature near the axis is about 9,000°K, very little N_2^+ would exist at this point. If the temperature near the boundary were about 6,000°K, one would expect a much greater N_2^+ concentration there. Looking across a diameter, one would then see both atomic and molecular lines each yielding a temperature characteristic of its region. Evidence that N_2^+ exists at the plasma boundary was cited in Section IV.

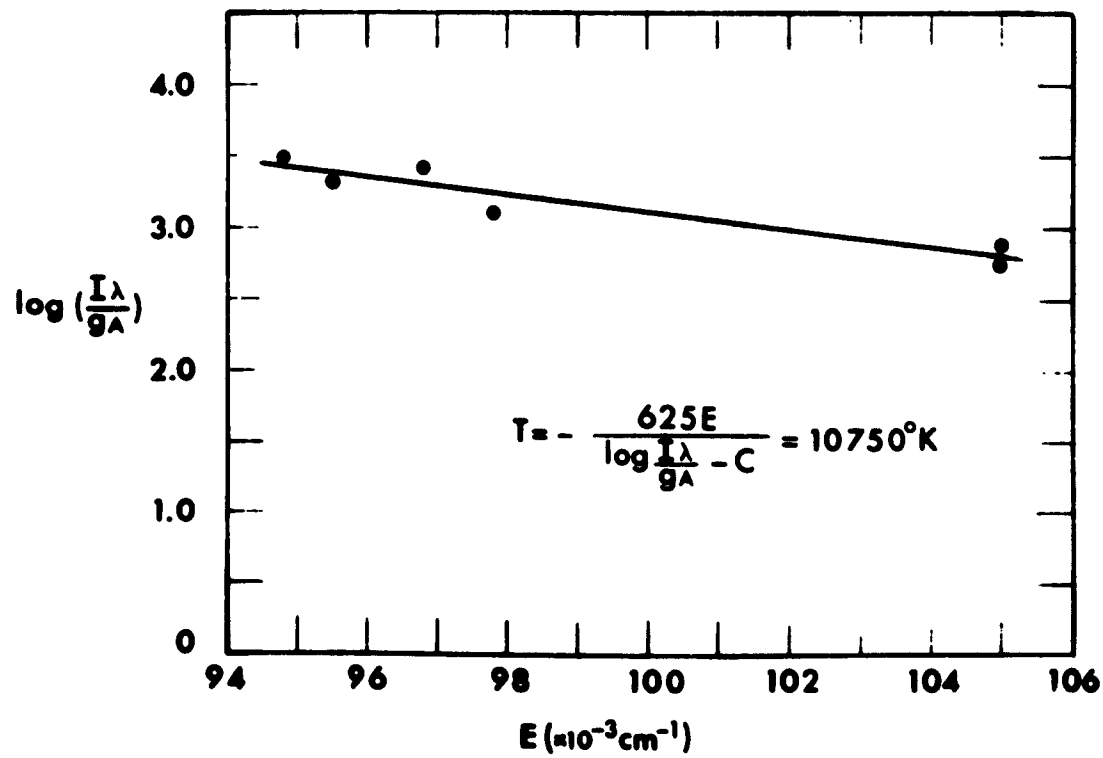

Fig. 13. Atomic Boltzmann plot for a nitrogen plasma, measured at 3/8" above the nozzle.

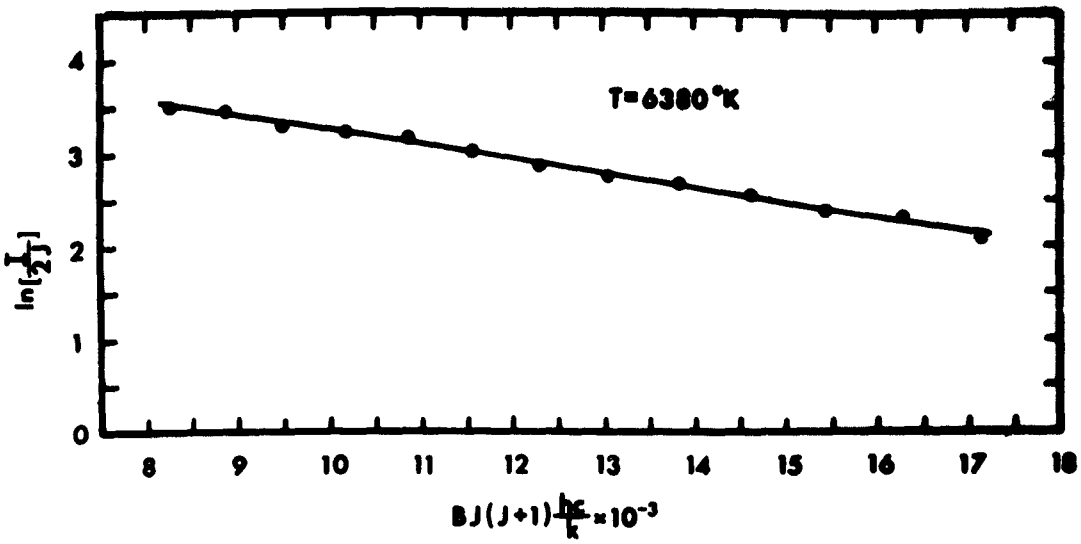

Fig. 14. Molecular Boltzmann plot for a nitrogen plasma, measured at 9/6" above the nozzle.

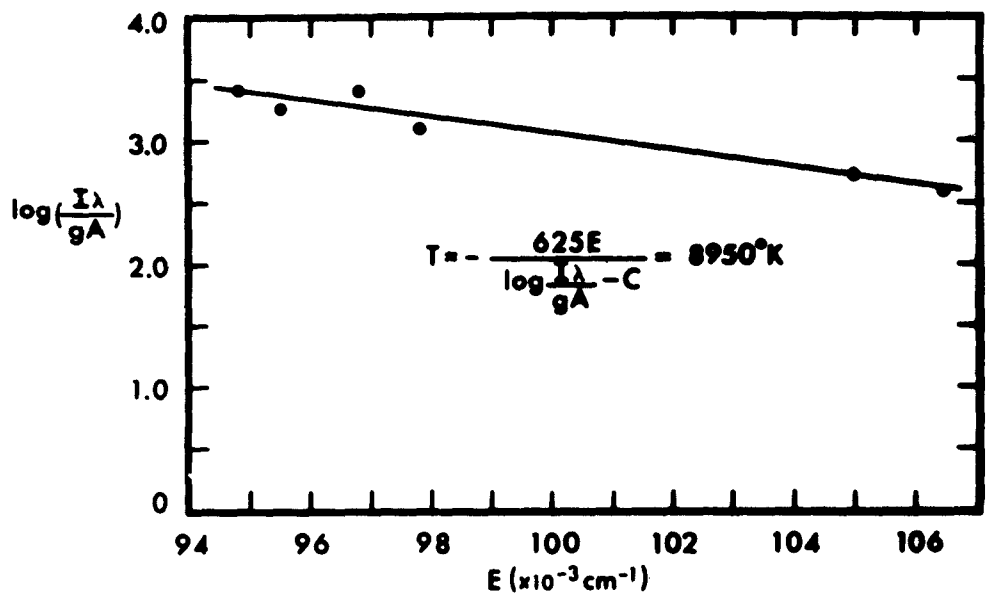

Fig. 15. Atomic Boltzmann plot for a nitrogen plasma, measured at 9/16" above the nozzle.

IMRA temperatures were measured at several lines of a nitrogen plasma. Figure 16 shows emission and absorption spectra from 0.90 - 1.05-u. Temperatures measured by the IMRA method have been written above each line in Fig. 16. Note that the temperature increases with decreasing wavelength. The same explanation applies that was given for the similar phenomenon with argon.

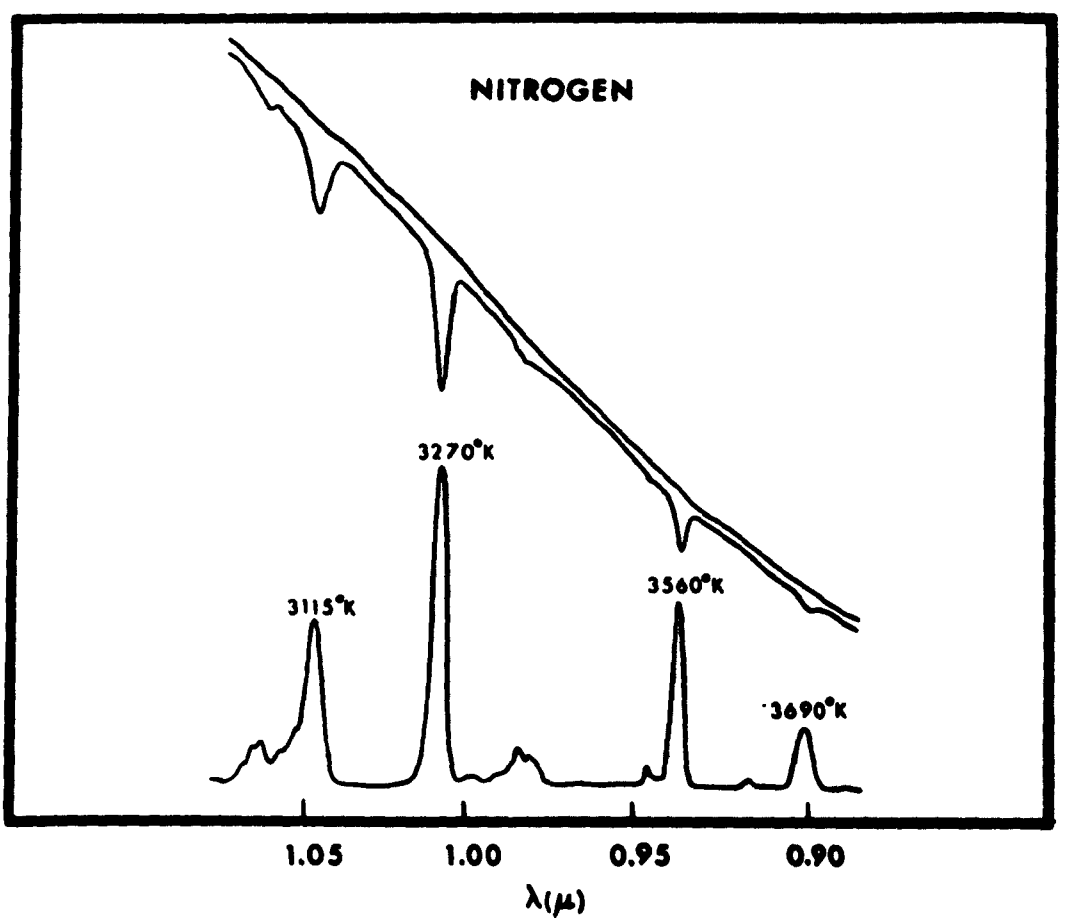

Fig. 16. Emission and absorption spectra of a nitrogen plasma, measured at 3/8" above the nozzle, showing IMRA temperatures.

D. Air.

Figure 17 shows emission and absorption spectra of an air plasma, and the corresponding IMRA temperatures. Because of experimental difficulties due to secondary arcing, the air plasma was less suitable for study than nitrogen. However, the two-line method may be used with much greater sensitivity with air than with nitrogen, because there are several pairs of oxygen lines for which the differences in upper energy states are considerable. For example, the 6157 Å and 3947 Å oxygen lines differ by 3.8 ev in upper energy levels. A calculation from these lines along a diameter 3/8" above the nozzle gave a temperature of 13,000°K.

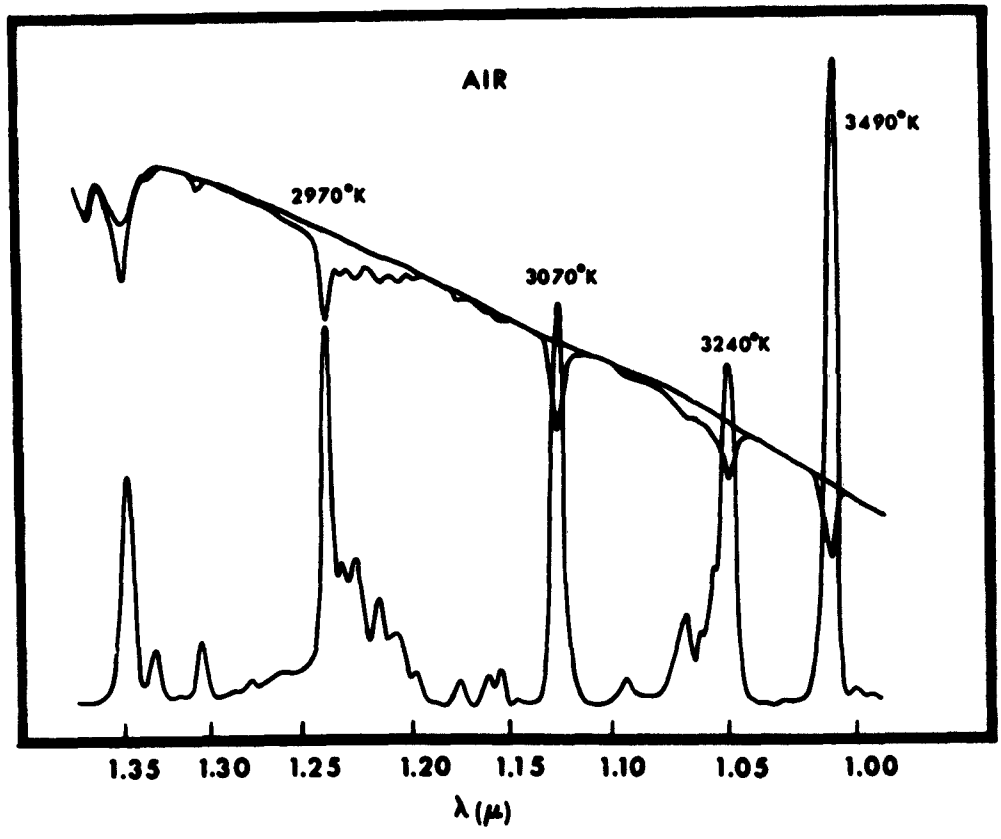

Fig. 17. Emission and absorption spectra of an air plasma, measured at 3/8" above the nozzle, showing IMRA temperatures.

E. Hydrogen and Helium.

The temperature of a hydrogen plasma was measured using the one-line method based on the Balmer H_α line. The peak temperature, determined in this way, was 8,580°K. The average hydrogen plasma temperature, determined by the IMRA method, was 3,340°K. The IMRA temperature determined from the 1.0829-μ helium line was 3,760°K. These results are tentative, since the hydrogen and helium plasmas were not studied extensively.

SECTION VI.

CONCLUSION

The principal results obtained in this study are summarized in Table II. Seeding a nitrogen plasmajet with argon allowed electron-excitation temperatures to be calculated simultaneously from argon and nitrogen atomic lines. The close agreement obtained was evidence that we were measuring the kinetic temperature, and provided verification of the one-line argon temperatures. The atomic Boltzmann plots verified the argon one-line temperatures, both in the nitrogen plasma and the pure argon plasma. It is noteworthy that the nitrogen temperature determined from the argon emission line was based on absolute intensity measurements, while the relative intensities of the nitrogen lines (in the atomic Boltzmann plot) were used to determine nitrogen temperature. Both measurements are strongly weighted toward the hot core of the plasmajet, where atomic concentrations are highest and molecular concentrations lowest. The molecular Boltzmann plot for nitrogen did not directly verify the single-line measurements, because the molecular Boltzmann temperature was weighted toward the outer boundary, where the concentration of dissociated N_2^+ was highest. However, the molecular temperature was consistent with our expectation that the coolest portion of the luminous plasma is at the boundary.(10).

It is quite obvious that plasmajets are characterized by large temperature gradients. The spectrometric measurement methods, which must use optically thin spectral lines, give results strongly weighted toward the peak temperature. The peak temperature is usually confined to a small region (10), and cannot be considered representative of the plasma as a whole. If radial symmetry exists, and if a lateral emission profile can be measured for an optically thin line of known transition probability, with known species concentration, then an Abelian integral inversion enables one to determine the radial temperature profile, but the results apparently exclude the effect of the relatively cool, outermost layer of the plasmajet. The IMRA method gives an average temperature, which can be weighted more or less toward

TABLE II.

Summary of Plasma Temperature Measurements by Various Methods

GAS	LOCATION Distance from Nozzle	METHOD of Temperature Measurement	TEMPERATURE
Nitrogen	3/8"	IMRA (NI lines)	3,115°-3,690°K
Nitrogen	3/8"	Molecular Boltzmann plot	Molecular lines too weak
Nitrogen	3/8"	Atomic Boltzmann plot	10,750°K
Nitrogen	3/8"	"One-line" method (Argon seeding)	10,950°K
Nitrogen	9/16"	Molecular Boltzmann plot	6,380°K
Nitrogen	9/16"	Atomic Boltzmann plot	8,950°K
Nitrogen	9/16"	"One-line" method (Argon seeding)	8,960°K
Argon	7/16"	Radial temperature plot[a)]	11,250°-14,400°K
Argon	7/16"	Lateral temperature plot[b)]	10,800°-12,850°K
Argon	9/16"	Radial temperature plot[a)]	10,750°-14,000°K
Argon	9/16"	Lateral temperature plot[b)]	9,800°-10,200°K
Argon	1"	Lateral temperature plot[b)]	8,100°-10,100°K
Argon	7/16"	IMRA (Ar I lines)	2,600°-8,000°K
Air	3/8"	IMRA (NI lines)	2,970°-3,490°K
Air	3/8"	"Two-line" method (OI lines)	13,000°K

a) Radial plots are based on the one-line method and the corresponding lateral temperature plot through the Abelian inversion formula.

b) Each point on a lateral temperature plot is calculated by the one-line method.

the peak, by judicious selection of wavelength. The IMRA measurements include the effect of the non-luminous sheath surrounding the visible plasmajet, which is not true of the spectrometric measurements. Currently available data are insufficient to evaluate this effect completely. When the inhomogeneous character of the plasmajet is taken into account, the results shown in Table II are consistent with each other.

All the methods of temperature measurement used here are useful tools for exploring the properties of plasmas. Further study is needed of the proper use of these tools. For this purpose, measurements in an isothermal plasma region are desirable, so that the measurement conditions will be well-defined and identical with respect to all the various measurement methods. Such measurements are planned for the near future.

APPENDIX. EQUIVALENCE OF THE "ONE-LINE" AND IMRA METHODS OF TEMPERATURE MEASUREMENT FOR AN OPTICALLY THIN PLASMA.

From the Planck law, the spectral emittance of a blackbody is given by

$$N_\nu d\nu = \frac{2hc^2\nu^3}{\exp\frac{c_2\nu}{T} - 1} d\nu \quad , \tag{1}$$

where $\nu = \frac{1}{\lambda}$. Let $\epsilon(\nu)$ be the emissivity of the plasma. Then

$$I_{em}d\nu = \epsilon(\nu)N_\nu d\nu = \frac{2hc^2\nu^3\epsilon(\nu)}{\exp\frac{c_2\nu}{T} - 1} d\nu \tag{2}$$

is the spectral emittance of the plasma. This can be written

$$I_{em}d\nu = \frac{c}{4\pi}\rho_\nu\epsilon(\nu)d\nu \tag{3}$$

where

$$\rho_\nu = \frac{8\pi\, hc\nu^3}{\exp\frac{c_2\nu}{T} - 1} \quad . \tag{4}$$

According to Kirchhoff's law and Lambert's law, emissivity is given by

$$\epsilon(\nu) = 1\text{-}e^{-k(\nu)L} \tag{5}$$

where L is the path length and $k(\nu)$ is the absorption coefficient. By definition, a line is optically thin if

$$0 \leq \epsilon(\nu) < 0.01$$

which implies that

$0 \leq k(\nu)L < 0.01005$ from the power series expansion of the exponential function in Eq. (5),

or,

$$\epsilon(\nu) \approx k(\nu)L \qquad (6)$$

for optically thin lines.

From Eq. (3) and Eq. (6) we get

$$I_{em}d\nu = \frac{c}{4\pi}\rho_\nu Lk(\nu)d\nu \quad . \qquad (7)$$

For a spectral line,

$$\nu_{nm} = \frac{E_n - E_m}{hc}$$

where E_n is the energy of the upper state and E_m is the energy of the lower state. With this notation, Eq. (4) and Eq. (7) can be written

$$\rho_\nu = \frac{8\pi hc\nu^3_{nm}}{\exp\frac{c_2\nu_{nm}}{T} - 1} \quad , \qquad (4')$$

and

$$I_{em}(\nu_{nm})d\nu = \frac{c}{4\pi}\rho_\nu\, Lk(\nu_{nm})d\nu \quad . \qquad (7')$$

For a system in radiative equilibrium, we have

$$N_nA_{nm} + N_nB_{nm}\rho_\nu = N_mB_{mn}\rho_\nu$$

where N_n and N_m are the number densities of atoms in energy states n and m, respectively, A_{nm} is the Einstein coefficient of spontaneous emission, B_{nm} is the Einstein coefficient of induced emission and B_{mn} is the Einstein absorption coefficient.

The net number of transitions from the lower state to the upper state due to the incident energy ρ_ν is

$$(N_mB_{nm} - N_nB_{nm})\rho_\nu,$$

so that

$$N_mB_{mn} - N_nB_{nm} = \frac{N_nA_{nm}}{\rho_\nu} \quad . \qquad (8)$$

The integrated absorption coefficient of a spectral line is given by

$$\int k(\nu)d\nu = (N_m B_{mn} - N_n B_{nm})h\nu_{nm} \quad . \qquad (9)$$

A result equivalent to Eq. (9) has been obtained by Crawford and Dinsmore (19). The integration of Eq. (7') and substitution of Eq. (9) into the resulting equation leads to

$$I_{em}^{nm} = \frac{c}{4\pi} \rho_\nu L(N_m B_{mn} - N_n B_{nm})h\nu_{nm} \quad , \qquad (10)$$

where

$$I_{em}^{nm} \equiv \int I_{em}(\nu)d\nu \quad .$$

The substitution of Eq. (8) into Eq. (10) results in

$$I_{em}^{nm} = L \frac{hc}{4\pi} N_n A_{nm} \nu_{nm} \quad .$$

This is Eq. (1) of Section II.

REFERENCES

1. R. H. Tourin, P. M. Henry, and E. T. Liang, J. Opt. Soc. Am. 51, 800 (1961).

2. R. H. Tourin, J. Heat Transfer 84, 164 (1962).

3. R. H. Tourin, P. M. Henry, and E. T. Liang, ARL 62-314, Part One of Final Report on Contract AF33(616)-6713, Aeronautical Research Laboratories, Wright-Patterson Air Force Base, Ohio (1961).

4. R. H. Tourin, Temperature, Its Measurement and Control in Science and Industry, Vol. III, C. M. Herzfeld, Editor (Reinhold Publishing Corp., New York, 1962), Part 2, Chap. 43.

5. R. H. Tourin and M. Grossman, Combustion and Flame 2, 330 (1958).

6. M. K. Jovanovic and D. R. Haworth, Oklahoma State Univ. (1960).

7. M. P. Freeman and S. Katz, J. Opt. Soc. Am. 50, 826 (1960).

8. M. N. Saha and B. N. Srivastava, Treatise on Heat (Hafner Publishing Co., New York, 1958).

9. C. F. Knopp, C. F. Gottschlich, and A. B. Cambel, Northwestern Univ., AFOSR Report 1100 (1961).

10. W. K. McGregor, Jr., M. T. Dooley, and L. E. Brewer, AEDC-TR-61-16 (1962).

11. W. J. Pearce, Optical Spectrometric Measurements of High Temperatures, P. J. Dickerman, Editor (Univ. of Chicago Press, 1960), p. 125.

12. W. F. Meggers, C. H. Corliss, and B. F. Scribner, NBS Monograph 32 (1961).

13. C. H. Corliss, J. Research Natl. Bur. Standards 66A, 5 (1960).

14. G. Herzberg, Spectra of Diatomic Molecules, 2nd Edition (D. Van Nostrand, New York, 1950), p. 204.

15. R. Herman and R. F. Wallis, J. Chem. Phys. 23, 637 (1955).

16. W. S. Benedict, private communication, 1962.

17. H. W. Drawin, Z. Physik 146, 295 (1956).

18. J. Richter, Z. Astrophysik 51, 177 (1961).

19. B. L. Crawford and H. L. Dinsmore, J. Chem. Phys. 18, 983 (1950); 18, 1682 (1950).

Aeronautical Research Laboratories, Wright-Patterson AFB, O. INFRARED SPECTRA AND TEMPERATURES OF PLASMAJETS: SPECTROMETRIC AND SPECTRORADIOMETRIC MEASUREMENTS OF PLASMAJET TEMPERATURE DISTRIBUTIONS by Lowell R. Ryan, Harold J. Babrov, Richard H. Tourin Warner and Swasey Co., Flushing N.Y. February 1963. 36 p. incl. illus. (Project 7063;Task 7063-01) (Contract AF 33(616)-8057 (ARL 63-35)

Unclassified Report

Temperatures of plasmajets were measured by several optical methods and the results intercompared. Both spectrometric and spectroradiometric methods

(over)

UNCLASSIFIED

were used. Argon and nitrogen plasmajet temperatures were studied in particular detail. Large temperature gradients were observed in all plasmajets studied. Spectra of plasmas were measured in both emission and absorption over the spectral range 0.37 to 5.0μ. Substantial emission was observed throughout the entire region. All the plasmas proved to be optically thick (measurable absorption) in the region of 0.7 - 2.0μ and optically thin (no absorption) in the region 0.37 - 0.7μ.

UNCLASSIFIED

Aeronautical Research Laboratories, Wright-Patterson AFB, O. INFRARED SPECTRA AND TEMPERATURES OF PLASMAJETS: SPECTROMETRIC AND SPECTRORADIOMETRIC MEASUREMENTS OF PLASMAJET TEMPERATURE DISTRIBUTIONS by Lowell R. Ryan, Harold J. Babrov, Richard H. Tourin Warner and Swasey Co., Flushing N.Y. February 1963. 36 p. incl. illus. (Project 7063;Task 7063-01) (Contract AF 33(616)-8057 (ARL 63-35)

Unclassified Report

Temperatures of plasmajets were measured by several optical methods and the results intercompared. Both spectrometric and spectroradiometric methods

(over)

UNCLASSIFIED

were used. Argon and nitrogen plasmajet temperatures were studied in particular detail. Large temperature gradients were observed in all plasmajets studied. Spectra of plasmas were measured in both emission and absorption over the spectral range 0.37 to 5.0μ. Substantial emission was observed throughout the entire region. All the plasmas proved to be optically thick (measurable absorption) in the region of 0.7 - 2.0μ and optically thin (no absorption) in the region 0.37 - 0.7μ.

UNCLASSIFIED